

Article

On the Radiolytic Stability of Potentiometric Sensors with Plasticized Polymeric Membranes

Julia Savosina^{1,2}, Marina Agafonova-Moroz^{1,2}, Maria Khaydukova¹ , Andrey Legin^{1,3}, Vasiliy Babain¹, Peter Tolstoy¹  and Dmitry Kirsanov^{1,3,*} 

¹ Institute of Chemistry, Saint-Petersburg State University, Peterhof, Universitetsky Prospect, 26, 198504 Saint-Petersburg, Russia; july-s@khlopin.ru (J.S.); ma-m@khlopin.ru (M.A.-M.); khaydukova.m@gmail.com (M.K.); a.legin@spbu.ru (A.L.); babainv@mail.ru (V.B.); peter.tolstoy@spbu.ru (P.T.)

² Khlopin Radium Institute, 2 Murinsky Prospect, 28, 194021 Saint-Petersburg, Russia

³ Laboratory of Artificial Sensory Systems, ITMO University, Kronverksky Prospect, 49, 197101 Saint-Petersburg, Russia

* Correspondence: d.kirsanov@gmail.com

Abstract: There is not much known on the stability of plasticized polymeric sensor membranes against ionizing radiation. While recent studies have indicated the applicability of potentiometric sensors with such membranes for quantification of actinides and lanthanides in spent nuclear fuel reprocessing solutions, the real industrial application of such sensors will require their stability in ionizing radiation fields. The present study explores this problem and evaluates the stability of potentiometric sensitivity towards lanthanides and actinides for a variety of plasticized polymeric membranes based on different neutral ligands. We demonstrate that most of the studied sensor compositions retain their sensitivity up to 50–100 kGy of the absorbed gamma radiation dose. The higher doses lead to the gradual loss of sensitivity due to the radiolysis of ligands and a polymer membrane matrix as confirmed by electrochemical impedance and nuclear magnetic resonance studies.

Keywords: potentiometric sensors; radiolytic stability; plasticized polymeric membranes; lanthanides; actinides; spent nuclear fuel



Citation: Savosina, J.; Agafonova-Moroz, M.; Khaydukova, M.; Legin, A.; Babain, V.; Tolstoy, P.; Kirsanov, D. On the Radiolytic Stability of Potentiometric Sensors with Plasticized Polymeric Membranes. *Chemosensors* **2021**, *9*, 214. <https://doi.org/10.3390/chemosensors9080214>

Academic Editor: Jose Vicente Ros Lis

Received: 8 July 2021

Accepted: 6 August 2021

Published: 8 August 2021

Publisher's Note: MDPI stays neutral with regard to jurisdictional claims in published maps and institutional affiliations.



Copyright: © 2021 by the authors. Licensee MDPI, Basel, Switzerland. This article is an open access article distributed under the terms and conditions of the Creative Commons Attribution (CC BY) license (<https://creativecommons.org/licenses/by/4.0/>).

1. Introduction

Potentiometric sensors with polymer plasticized membranes are popular analytical instruments that have found massive application in various fields [1–3] due to very simple measuring procedure, low cost and low detection limits for a variety of ions. These sensors are also widely employed in multisensor arrays (so called “electronic tongues”) for qualitative and quantitative analysis of complex liquids [4].

Recently, a new application of multisensor systems was proposed related to a very challenging task of actinides and lanthanides quantification in technological solutions of spent nuclear fuel (SNF) reprocessing [5–7]. The analytical chemistry of such media is not trivial at all due to the following reasons. Firstly, the composition of these solutions includes almost the whole periodic table of elements. Secondly, during the most common industrial reprocessing scheme PUREX (Plutonium-URanium Extraction), the SNF is dissolved in highly concentrated nitric acid and the media is chemically aggressive. Thirdly, the radioactive fission products in the media yield a high level of radioactivity. In these circumstances, the options for real-time chemical analysis of the SNF reprocessing streams are very limited. Most of the analytical procedures routinely employed in this field require sampling and tedious sample preparation (e.g., inductively coupled plasma atomic emission spectrometry) [8].

The necessity of safe process management leads to the search for the analytical methods that would be capable of quantifying the key SNF components directly in technological

streams in on-line mode. Up to now there were only two suitable approaches suggested: optical spectrometry with chemometric data processing [9,10] and electrochemical multisensor systems [6,7]. While optical spectrometry with fiber probes indeed allows quite precise analysis of certain components in SNF solutions, it may suffer from light scattering effects observed in these solutions due to gas formation and the presence of colloid particles. Moreover, the detection limits of optical spectrometry in direct mode (without using dyes) are in some cases not sufficient for this task. These issues lead to the development of potentiometric sensor arrays that would be capable of on-line analysis of target analytes. While the applicability of this approach was already demonstrated in both model mixtures [5,6] and real industrial samples [7], there are still some issues hindering immediate industrial implementation of the methodology. One of the most important problems relates to the stability of sensing properties of polymer plasticized membranes when exposed to continuous ionizing radiation that will be an unavoidable factor when dealing with real industrial application. The exposure of polymeric materials to radiation is known to result in changes in molecular structure of polymers and consequently their chemical and physical properties [11,12]. The same is expected to happen with polymer plasticized sensor membranes; however, the particular values of absorbed doses that will lead to the loss of electrochemical sensing properties are not clear.

At the moment, only scarce information about possible effects of radiation on ion-selective sensors is available in literature [13,14]. The report [13] studied several glass electrodes, calomel electrodes, fluoride-selective single crystal electrodes and nitrate-selective electrodes with liquid ion-exchangers. The response of the calomel electrode was not affected by gamma radiation (up to 1 MGy accumulated dose). Small potential shifts after certain times were attributed to the temperature effects induced by sample heat-up under a radiation field. Fluoride and glass electrodes have also demonstrated little susceptibility to gamma radiation. The nitrate electrode was also stable up to the cumulative doses of 1 kGy, while higher doses induced small parallel shifts of the response curve. These shifts become non-linear at 1 MGy, however the linearity was restored by changing the internal reference solution. The author observed color changes in the liquid ion exchanger—it became dark colored after a large dose—as well as the plastic electrode body. The paper [14] explored H⁺ and Na⁺-selective glass membrane electrodes and polycrystalline Cl⁻-selective electrodes. The authors observed the shifts of electrode potentials upon exposure to a gamma-radiation field. The shifts varied in the range 20–100 mV depending on the radiation intensity and electrode membrane resistance. The shifts were reversible and the electrode potential offsets were eliminated by stopping irradiation. The authors attributed these variations to radiation-induced currents in coaxial cables. Neither study [13] nor study [14] explored the radiation-induced changes in electrode membrane materials upon accumulation of certain doses.

The purpose of the present research was to explore the influence of ionizing radiation on the electrochemical sensitivity of the potentiometric sensors with plasticized polymeric membranes and to investigate the type of chemical changes in these materials upon radiation. The sensors with pronounced sensitivities towards lanthanides and actinides were studied to explore their applicability in industrial conditions for continuous SNF reprocessing monitoring.

2. Materials and Methods

2.1. Potentiometric Sensors

The sensors for the study were chosen among those previously developed for quantification of lanthanides and actinides in SNF process streams [5,6]. Table 1 shows the chemical structures of the employed ligands. All the ligands were purchased from Sorbent Technologies, LLC (Moscow, Russia). Plasticized polymeric sensor membranes were prepared using conventional procedures. The weighted amounts of membrane components were dissolved in freshly distilled tetrahydrofuran and poured into flat Teflon beakers. The cocktails were left overnight for tetrahydrofuran evaporation. After

that, sensor membranes 4 mm in diameter were cut from the parent membrane of each composition and glued upon the end of PVC sensor bodies with PVC-cyclohexanone mixture. Each sensor membrane contained 50 mmol/kg of ligand. High molecular weight poly(vinylchloride) (Merck, Darmstadt, Germany) was used as a polymer (PVC) and 2-nitrophenyl octyl ether (NPOE) as a solvent-plasticizer. Two different substances were employed as cation-exchangers, both in 10 mmol/kg concentration: sodium tetrakis [3,5-bis(trifluoromethyl)phenyl]borate (TFPB) or acidic form of chlorinated cobalt dicarbollide (CCD). TFPB was procured from Merck (Darmstadt, Germany), CCD was kindly provided by Catchem (Czech Republic).

Table 1. Chemical structures of the employed ionophores.

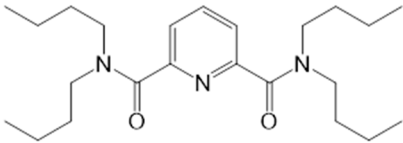
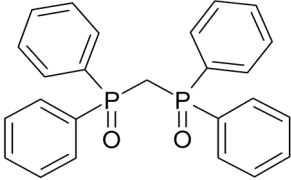
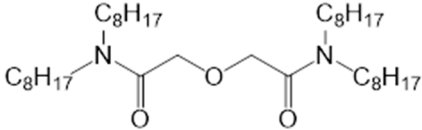
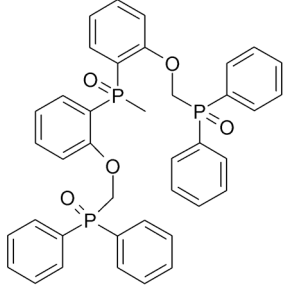
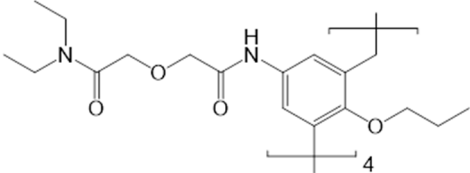
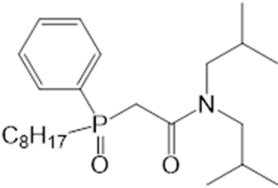
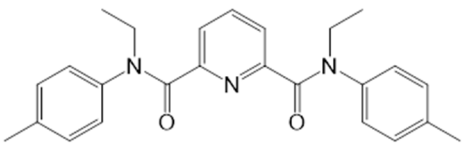
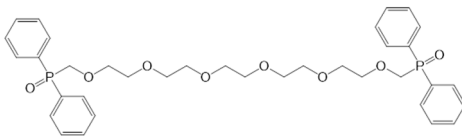
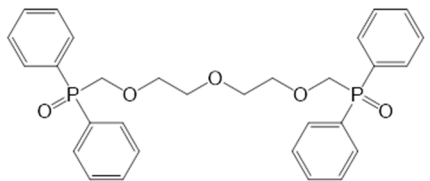
Sensor	Ionophore	Chemical Structure	Cation Exchanger
i1		<i>N,N',N,N'</i> -Tetrabutylamide of dipicolinic acid	TFPB
i2		Tetraphenylmethylene diphosphine dioxide	TFPB
i3		<i>N,N',N',N'</i> -Tetraoctyldiamide of diglycolic acid	CCD
i4		1,9-Bis-(diphenylphosphinyl)-3,6-dibenzo-2,8-dioxa-5-methylphosphineoxanonane	TFPB
i5		5,11,17,23-Tetra(diethylcarbamoyl)-ethoxymethylcarboxamido)-25,26,27,28-tetrapropoxycalix[4]aren	CCD
i6		Phenylloctyl- <i>N,N</i> -di- <i>iso</i> -butylcarbamoyl-methylen phosphine oxide	CCD

Table 1. Cont.

Sensor	Ionophore	Chemical Structure	Cation Exchanger
i7		<i>N,N'</i> -Diethyl- <i>N,N'</i> -di- <i>p</i> -tolylidiamide of dipicolinic acid	TFPB
i8		1,18-Bis-(diphenylphosphanyl)-2,5,8,11,14,17-hexaoxaoctadecane	CCD
i9		1,9-Bis-(diphenylphosphanyl)-2,5,8-trioxanonane	CCD

Two identical sensor arrays were prepared: one was used for irradiation and one was used as a control. All sensors were conditioned for 48 h in 0.01 M NaCl prior to measurements.

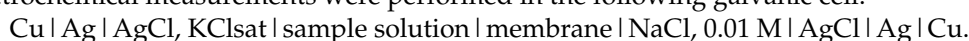
2.2. Sensor Irradiation

The physicochemical consequences of all types of irradiation (alpha, beta and gamma) are rather similar, hence the name “ionizing radiation”. Alpha-radiation is normally not employed for radiation stability studies due to very low permeation ability and physical difficulties in organizing appropriate and standardized conditions. While the permeation ability of beta-radiation is higher, it is hard to find appropriate standardized sources of sufficiently intense beta-radiation. Thus, gamma-radiation is a standard approach to study radiation stability of various materials.

The sensors were irradiated with ^{60}Co gamma radiation set-up K-120000 (Peter the Great Polytechnic University, St. Petersburg, Russia) with radiation intensity 20 kGy/h. Several radiation sessions were taken until the accumulated dose of 442.5 kGy was reached. The sensors were placed in the radiation chamber on the special shelf where exact cumulative dose can be calculated based on the distance from the ^{60}Co radiation source and surrounding chamber geometry. In order to explore the influence of radiation on the chemical structures of the membrane active compounds, the nitrobenzene solutions of two ligands *N,N',N,N'*-tetrabutylidiamide of dipicolinic acid (**i1**) and phenyloctyl-*N,N*-di-*iso*-butylcarbamoyl-methylen phosphine oxide (**i6**) as typical nitrogen- and phosphorus-containing ligands were prepared. For this purpose, 50 mg of ligand were dissolved in 0.5 mL of nitrobenzene. Nitrobenzene was employed as a less viscous analogue of NPOE. The solutions were placed into polyethylene vials with gas-tight caps of 2 mL total volume and placed in the chamber to accumulate a total dose of 442.5 kGy. Similar solutions containing secondary amines di(*n*-butyl)amine and di(*iso*-butyl)amine were prepared as these substances were supposed to be the radiolysis products of the amide groups in the ligands according to [15].

2.3. Potentiometric Measurements

After each irradiation session the potentiometric sensitivity of the sensors towards typical lanthanides and actinides in SNF media (Pr^{3+} , Gd^{3+} and UO_2^{2+}) was studied. Electrochemical measurements were performed in the following galvanic cell:



Ag/AgCl reference electrode EVL 1M 3.1 (ZIP, Gomel, Belorussia) was applied. Sensor potentials were registered using a KHAN-32 (Sensor Systems, LLC, St. Petersburg, Russia) high impedance 32-channel digital mV-meter with 0.1 mV accuracy. The mV-meter was connected to a PC for data acquisition and processing. The sensor sensitivities were studied in aqueous solutions containing 10^{-7} to 10^{-3} M of individual ions. The solutions were prepared by subsequent dilution from 0.1 M stock solutions of Me^{3+} nitrates (Sigma-Aldrich, Germany) or $\text{UO}_2(\text{NO}_3)_2 \cdot 6\text{H}_2\text{O}$ (JSC Isotope, Moscow, Russia). The slopes of the linear parts of the calibration curves were averaged over three repetitions. All potentiometric measurements were carried out in nitric acid solutions at pH 2 to suppress metal hydrolysis. After each set of measurements, the sensors were washed with several portions of double distilled water to reach the initial and stable readings in water.

2.4. Electrochemical Impedance Measurements

Electrochemical impedance measurements were performed using potentiostat/galvanostat Reference 600R (Gamry Instruments, Warminster, PA, USA). Electrochemical impedance spectra (EIS) were registered in the frequency range from 150 Hz to 1 MHz. Alternating current voltage was 100 mV. Impedance measurements were carried out in the three electrode cell with electrolytic contact. The sensors with PVC membranes were equipped with internal reference Ag/AgCl electrode and filled with 0.01 M NaCl. A standard Ag/AgCl electrode (1004G, Gamry Instruments) was used as a reference electrode. Pt foil (0.7 cm^2) was used as a counter electrode. All the electrodes were firmly fixed in the cover of the glass cell filled with 0.01 M NaCl. The cell with all connectors and cables was placed in the Faraday cage. The measurements were done at room temperature. The processing of the spectra was performed in Gamry Echem Analyst software package (Gamry Instruments, Warminster, PA, USA).

2.5. NMR Spectroscopic Measurements

A nitrobenzene solution of 0.5 mL of each ligand was put in contact with 0.5 mL of distilled water and rigorously shaken for 3 min. After separation of the water layer, it was decanted. This was done since the water molecules are one of the major sources of active radicals contributing to radiation damages. Since the sensors are operating in the aqueous media, this procedure is necessary to ensure comparable conditions of radiolysis. The resulting water content differed from sample to sample and was not controlled precisely, though it was similar in all studied samples. After that, 0.5 mL of the resulting nitrobenzene solution of each ligand was placed in a standard 5 mm NMR sample tube into which a glass capillary filled with D_2O (99.8% D, abcr GmbH) was then placed. The samples containing the solutions of secondary amines (di(*iso*-butyl)amine and di(*n*-butyl)amine) were prepared in a similar way. These solutions were prepared to confirm the expected radiation-induced decomposition products of two ligands (**i1** and **i6**).

The liquid-state ^1H NMR spectra were recorded at the Center for Magnetic Resonance (Saint-Petersburg State University Research Park) on Bruker Avance III 500 MHz NMR spectrometer (11.74 T, 500.03 MHz for ^1H). The acquisition parameters were as follows: 30° -pulses, acquisition time 3.3 s, the relaxation delay 1.0 s, number of scans 16. The magnetic field was stabilized (locked) and ^1H NMR spectra were calibrated to tetramethylsilane (TMS) scale using the deuterium signal of D_2O in capillary as an external standard. The calibration was done using the unified Ξ scale according to IUPAC recommendations [16].

3. Results and Discussions

3.1. Potentiometric Measurements

The potentiometric sensors were irradiated step by step in the gamma-camera and the calibration measurements of the sensors between the irradiations were performed in the nitric acid solutions of Pr^{3+} , Gd^{3+} and UO_2^{2+} at pH 2. The content of the metal ions was varied in the range 10^{-7} – 10^{-3} M. Figure 1 shows the typical evolution of the calibration curves in Pr^{3+} solutions using the sensor based on carbamoyl phosphine oxide (**i6**) as

an example. One can see that with the growth of the accumulated dose, the sensitivity is gradually decreasing and falls to the impracticably low values at the maximal dose of 442.5 kGy. In general, a similar trend was observed for all studied sensors. Table 2 summarizes the determined potentiometric sensitivity values for all of the sensors and all the studied ions.

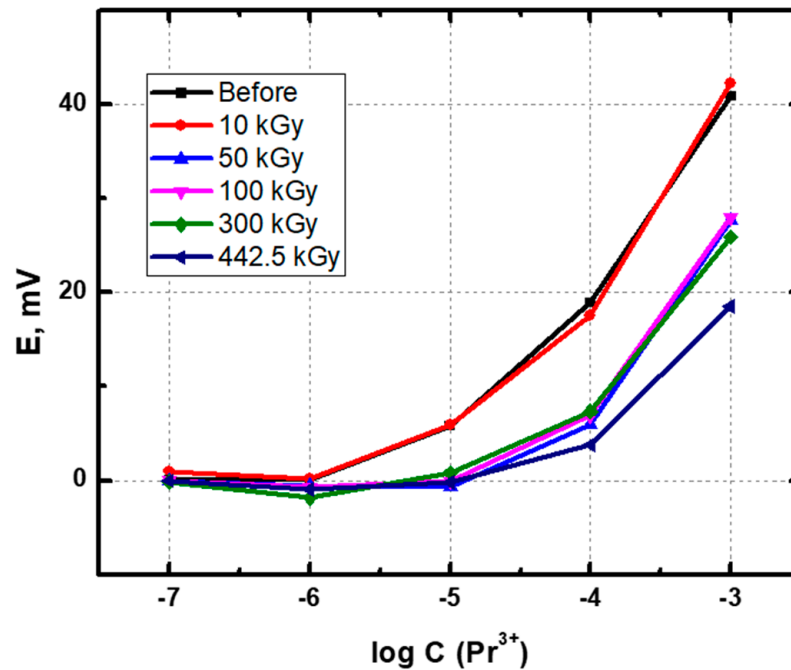


Figure 1. The response curves of the sensor i6 before and after the accumulation of the different absorbed radiation doses.

Table 2. Potentiometric sensitivity of the sensors after accumulation of various absorbed radiation doses (± 1 mV/dec).

Absorbed Radiation, kGy	Pr ³⁺								
	i1	i2	i3	i4	i5	i6	i7	i8	i9
0	15	3	5	4	17	18	15	11	7
10	18	5	7	5	18	18	15	10	11
50	12	5	7	6	17	19	9	11	10
100	13	2	6	5	19	18	8	13	9
300	8	5	7	7	18	19	2	5	9
442.5	4	3	8	4	18	19	1	-7	6
Absorbed Radiation, kGy	Gd ³⁺								
	i1	i2	i3	i4	i5	i6	i7	i8	i9
0	16	12	15	9	15	17	19	13	10
10	15	-2	10	2	12	15	19	9	9
50	12	-5	12	1	11	13	13	12	9
100	12	-3	10	3	8	10	11	11	7
300	5	-2	11	1	4	7	2	1	4
442.5	6	-2	13	4	0	7	3	0	3

Table 2. Cont.

	UO ₂ ²⁺								
0	18	23	−2	21	12	64	20	9	21
10	20	23	−1	22	6	59	29	11	19
50	16	18	−2	19	7	50	19	13	21
100	14	18	0	18	5	46	18	10	16
300	9	8	−1	16	2	39	8	10	13
442.5	8	12	1	14	−1	37	9	2	10

A clear dependence of the sensitivity loss on the sensor membrane composition can be seen. For example, the sensor **i1** based on *N,N',N,N'*-tetrabutylamide of dipicolinic acid has almost completely lost its sensitivity for Pr³⁺ already after accumulation of 100 kGy, while the sensors **i4** (based on 1,9-Bis-(diphenylphosphynyl) 3,6-dibenzo-2,8-dioxo-5-methyl-phosphineoxanonane) in the case of Gd³⁺ and **i8** (based on 1,18-Bis-(diphenylphosphynyl)-2,5,8,11,14,17-hexaoxaoctadecane) in the case of uranyl remain functioning even after the accumulation of 442.5 kGy. This may imply somewhat better radiolytic stability of the sensors based on phosphoryl-containing podands compared to diamides. In general, for most of the sensors a significant decrease in sensitivity can be observed at an accumulation of 50–100 kGy. The distinct super-Nernstian sensitivity of **i6** (based on phenyloctyl-*N,N*-di-*iso*-butylcarbamoyl-methylen phosphine oxide) in uranyl solutions can be in part attributed to the high affinity of the ligand towards uranyl and non-equilibrium measurement conditions (NaCl in the inner solution).

At the same time the control set of sensors which was not subjected to the gamma irradiation did not show a decrease of sensitivity in the period of the experiment. The corresponding values are given in Table S1 (Supplementary Materials).

Besides the changes in response curve slopes the offsets in potential values of the sensors were also observed upon the irradiation (Figure 2). While some of the sensors demonstrated reasonably smooth behavior of potential values, the others exhibited abrupt changes. No such effects were observed for the control sensor array where corresponding values were mostly fluctuating around quasi-stable numbers ± 10 mV. We attribute the changes in sensitivities and absolute EMF (electromotive force) values to the chemical damages induced by gamma radiation in plasticized polymeric sensor membranes. In line with a previous observation on nitrate-selective membrane electrodes [13], we observed the change in color for both the sensing membranes and PVC electrode bodies (Figure 3). The irradiated sensors became much darker.

In general, it can be concluded that in most cases the polymeric sensor membranes retain their sensitivity towards lanthanides and uranyl ions up to 100 kGy of absorbed radiation dose. Taking into account radiation burdens typical for various stages of SNF reprocessing, this stability is enough to ensure continuous sensor application in these media for at least 1 month, depending on the radioactivity of the analyzed media. For certain stages of the process, this radiolytic stability will be sufficient for 10–12 months of continuous working.

In order to get some insights into the irradiation consequences, we have conducted two additional series of studies. First, the irradiated sensor membranes were studied with electrochemical impedance to check the overall changes in electrical resistance. Second, model solutions of two ligands in nitrobenzene that were irradiated with 442.5 kGy dose were studied by NMR spectroscopy to discover possible chemical consequences of irradiation in ligand structure.

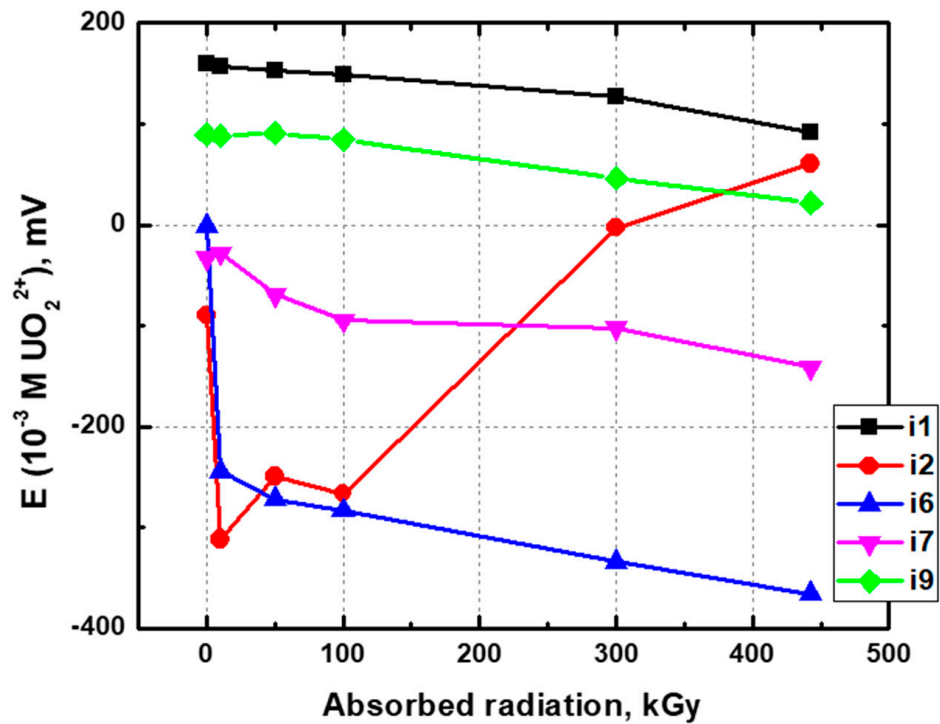


Figure 2. Typical evolution of sensor potentials in 10^{-3} M uranyl nitrate solution after the accumulation of the different absorbed radiation doses (the readings of i9 are shifted 60 mV down for better visibility).



Figure 3. The visual appearance of the studied sensor arrays after exposure to gamma radiation (left) and without exposure (right).

3.2. Electrochemical Impedance Measurements

In most cases, the radiation induced damage in membrane structure led to a significant increase in membrane resistance. Before the impedance measurements both sets of sensors (irradiated and control) were washed with distilled water and soaked in 0.01 M NaCl for

3 days. After that, the sensors were refilled with fresh internal solution and immersed in 0.01 M NaCl for 1 h. This strategy was chosen since irradiated sensor membranes have demonstrated continuous variation in electrical resistance upon membrane soaking. Probably, this can be attributed to the strong ion uptake by these membranes, associated with the increased ion-exchange capacity upon irradiation due to the appearance of novel ion-exchanging sites. As an example, Figure S1 (Supplementary Material) shows the evolution of **i8** membrane resistance upon soaking in 0.01 M NaCl. At the same time the non-irradiated membrane has shown reasonably stable electrical resistance values. This can be an indication of radiation effects that led to the changes in the physical membrane structure at the micro level and resulted in such unstable behavior. Longer soaking resulted in further decrease down to hundreds kOhm values; however, after overnight drying on air the resistance increased again. Figure S2 (Supplementary Material) shows the Nyquist plots for irradiated and non-irradiated **i8** membranes. The equivalent circuit used to fit the data and corresponding components of impedance-plane plot are also shown therein. We assume that obtained EIS spectra can be fitted by constant phase element with diffusion, but the Warburg element cannot be seen due to the range of the frequencies. This unstable behavior of the irradiated membranes does not allow a reliable direct comparison of electrical resistance values of two sensor arrays; nevertheless, some rough estimates can be done. Figure 4 shows the membrane resistance values for irradiated and control membranes. In the case of irradiated membranes, the values calculated from EIS spectra after 1 h soaking in 0.01 M NaCl are shown. No error bars are given in this case due to continuous evolution of these values upon soaking. Longer soaking may lead to a 2–3 fold decrease in resistance; however, this decrease is reversible upon drying. These data can only be considered on the qualitative level. Generally, in most of the cases we observe considerable increases in membrane resistance after gamma irradiation. The sensors **i4** and **i6** based on the ligands with phosphine oxide functionalities have shown smaller increases in impedance values. However, the membrane resistance values of the irradiated sensors were not stable in time (Figure S1) and responsible evaluation of the ligand effect in this case is hardly possible.

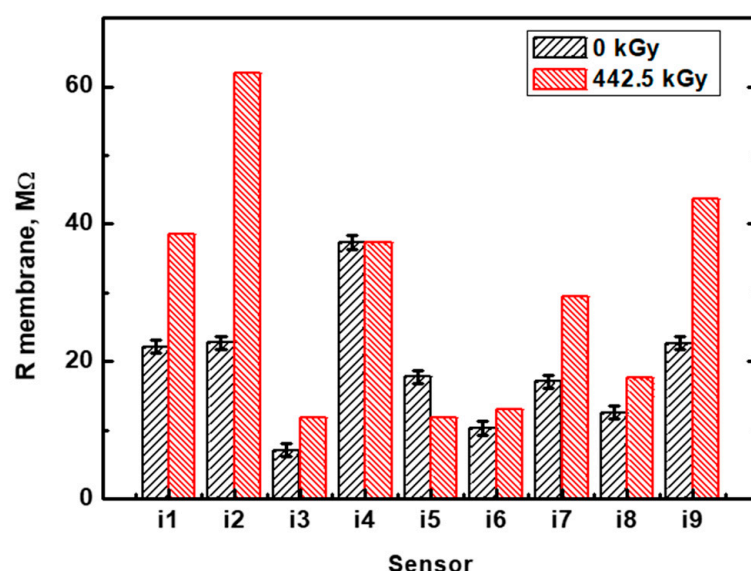


Figure 4. Membrane resistance for control (0 kGy) and irradiated (442.5 kGy) sensor arrays.

3.3. NMR Spectroscopic Measurements

In order to estimate the fraction of the ligand molecules damaged by the radiation dose and in order to characterize the main decomposition products, we have studied ^1H NMR spectra of **i1** and **i6** in nitrobenzene solution before and after the exposure to ionizing radiation. The overview of the resulting ^1H NMR spectra are shown in Figures S3 and S4

in Supplementary Material, while here for brevity we present and discuss only the spectral regions containing the signals of the protons which were most useful for the assignment and interpretation. In Figure 5, we compare the OH/NH proton signal regions for **i1** and **i6**, while in Figure 6 for **i1**, we show the aliphatic spectral region containing the signals of alkyl protons of the amide/amine substituents.

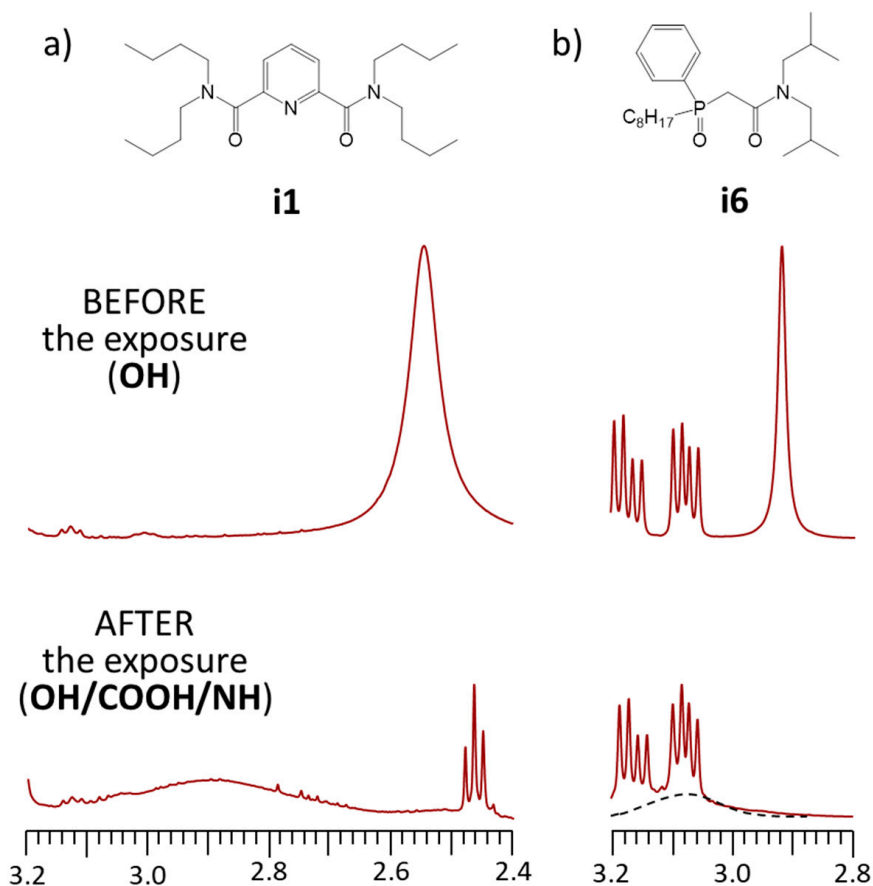


Figure 5. The parts of room temperature ^1H NMR spectra containing the OH/NH proton signals of nitrobenzene solutions of (a) **i1**, (b) **i6** before and after the exposure to ionizing radiation.

Figure 5 demonstrates that in each case after the exposure, the average signal of all the mobile protons is broadened and shifted to lower fields, indicating the formation of more acidic and less shielded mobile protons which are in exchange with the OH protons of water. In turn, Figure 6 shows that while before the exposure (Figure 6a) only the proton signals of two N-CH₂-CH₂-CH₂-CH₃ fragments are visible (the non-equivalency is caused by the hindered rotation around the amide bond), while after the exposure (Figure 6b), a new set of signals appears. The chemical shifts of some of the signals match those of butyl moieties in di(*n*-butyl)amine, measured separately (Figure 6c), while some other signals indicate the presence of unreacted amides. Thus, by combining the main observations from Figures 5 and 6, one could conclude that the primary effect of the exposure to ionizing radiation for **i1** is the hydrolysis of the amide bond with the formation of di(*n*-butyl)amine and the corresponding pyridinecarboxylic acid (containing the unreacted amide). The cleavage of the amide bond could be initiated either directly, after the absorption of a gamma quantum by the molecule, or indirectly via the initial radiolysis of water molecules.

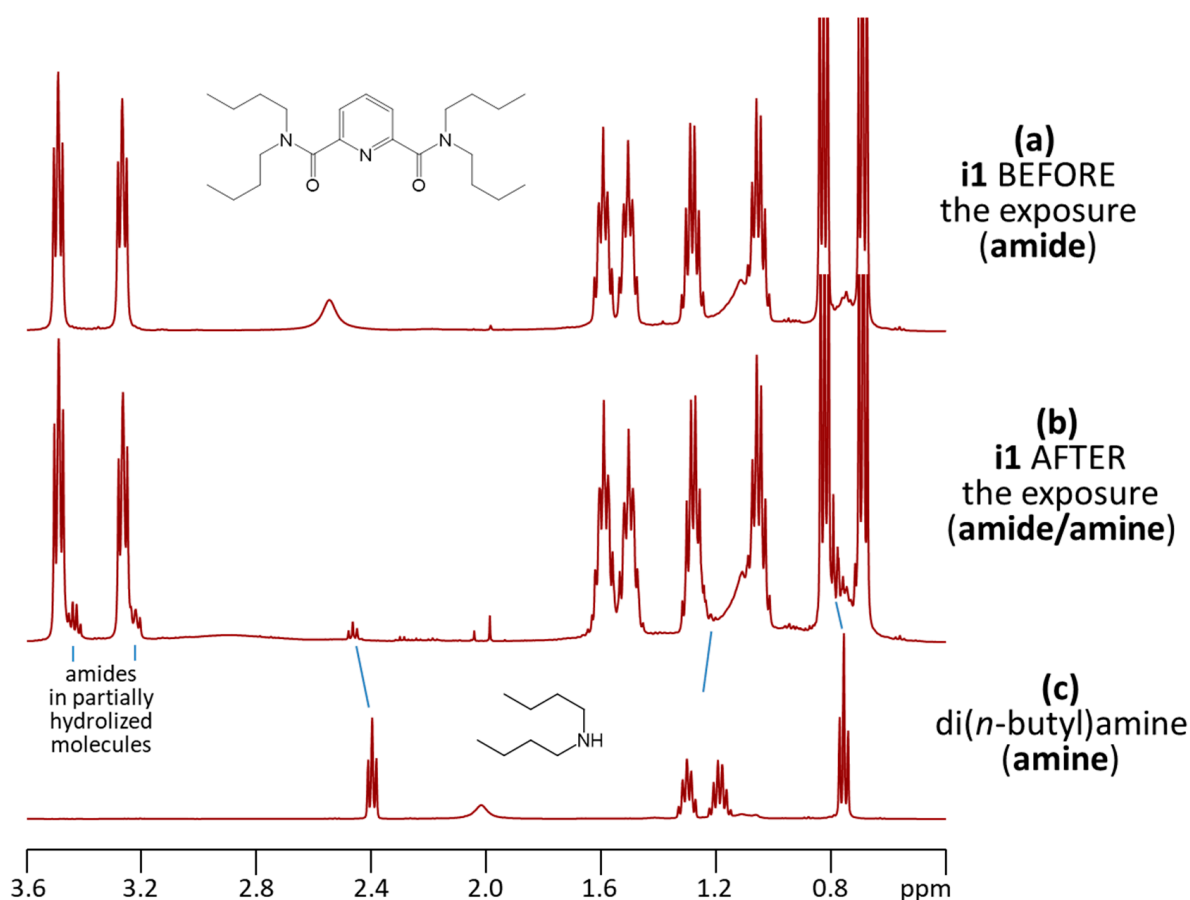


Figure 6. The aliphatic parts of room temperature ^1H NMR spectra containing the signals of alkyl protons of amide/amine substituents for nitrobenzene solutions of (a) *i1* before the exposure, (b) *i1* after the exposure, (c) di(*n*-butyl)amine.

One could use the ^1H NMR integrated signal intensities to estimate the fraction of the intact and reacted (partially hydrolyzed) *i1* molecules. Integration of strong and weak signals in the 3.6–3.2 ppm range gives the ratio 90:10; thus, ca. 10% of amide bonds were hydrolyzed. Assuming that hydrolysis of both amide bonds in one molecule is statistically unlikely, we could estimate that ca. $18 \pm 2\%$ of molecules were damaged by radiation. Most probably, the di(*n*-butyl)amine is not the only side product of the radiation damage, because the integral intensity of the small triplet at ca. 2.5 ppm, assigned to the N–CH protons of di(*n*-butyl)amine, is insufficient to account for the total amount of partially hydrolyzed molecules giving rise to the N–CH signals at 3.22 and 3.43 ppm.

4. Conclusions

The study of gamma irradiation effects on the electrochemical properties of plasticized polymeric membranes of potentiometric sensors revealed that these materials keep their functionality up to 50–100 kGy of the absorbed dose, depending on the particular ligand. Two possible reasons of deterioration of the sensing properties were detected. The first one is associated with the partial radiolysis of neutral ligands providing for potentiometric sensitivity. The second one is related to the radiation damage in membrane matrix highlighted by impedance measurements. Both phenomena may lead to the gradual loss of the electrochemical response and both of them are not recoverable with time due to their irreversible nature. Nevertheless, the evaluated stability of response is sufficient for continuous sensor application in SNF process streams for at least one month, which appears to be a reasonable lifetime when taking into account the complexity of the analytical task and the simplicity of multisensor systems.

Supplementary Materials: The following are available online at <https://www.mdpi.com/article/10.3390/chemosensors9080214/s1>, Table S1: Potentiometric sensitivity of the control sensor array during the experiment (± 1 mV/dec); Figure S1: The evolution of the i8 membranes' resistance upon soaking in 0.01 M NaCl; Figure S2: Nyquist plots the i8 membranes' resistance upon soaking in 0.01 M NaCl. Right after interaction with 0.01 M NaCl (0 h) and after immersion in the solution during 1–4 h (1–4 h), respectively. Equivalent circuit is schematically shown at the top of the figure, where R_{sol} —uncompensated solution resistance, CPE—constant phase element, R_m —bulk membrane, W_m —Warburg element. Calculated Nyquist plot based on the equivalent model circuit is shown as a black curve; Figure S3: (a) Overview of 1H NMR spectra of nitrobenzene solutions of i1 before and after the exposure to ionizing radiation. (b) The amplified aromatic and aliphatic parts of the same spectra (the most discernable new signals are marked by arrows). The bottom spectrum corresponds to the nitrobenzene solution of di(n-butyl)amine, measured separately; Figure S4: (a) Overview of 1H NMR spectra of nitrobenzene solutions of i6 before and after the exposure to ionizing radiation. (b) The amplified aromatic and aliphatic parts of the same spectra (the most discernable new signals are marked by arrows). The bottom spectrum corresponds to the nitrobenzene solution of di(iso-butyl)amine, measured separately.

Author Contributions: J.S.: Formal Analysis, Investigation, Data Curation; M.A.-M.: Formal Analysis, Investigation, Data Curation; M.K.: Validation, Formal Analysis, Investigation, Data Curation, Writing—Original Draft, Visualization; A.L.: Resources, Writing—Review and Editing, Project Administration; V.B.: Conceptualization, Writing—Original Draft; P.T.: Validation, Formal Analysis, Investigation, Data Curation, Writing—Original Draft, Writing—Review and Editing; D.K.: Conceptualization, Methodology, Formal Analysis, Data Curation, Writing—Original Draft, Writing—Review and Editing, Visualization, Supervision, Project Administration. All authors have read and agreed to the final version of the manuscript.

Funding: This study was supported by Russian Science Foundation grant #18-19-00151.

Conflicts of Interest: The authors declare no conflict of interest.

References

1. Crespo, G.A. Recent advances in ion-selective membrane electrodes for in situ environmental water analysis. *Electrochim. Acta* **2017**, *245*, 1023–1034. [[CrossRef](#)]
2. Parrilla, M.; Cuartero, M.; Crespo, G.A. Wearable potentiometric ion sensors. *TrAC Trends Anal. Chem.* **2019**, *110*, 303–320. [[CrossRef](#)]
3. Özbek, O.; Berkel, C.; Isildak, Ö. Applications of potentiometric sensors for the determination of drug molecules in biological samples. *Crit. Rev. Anal. Chem.* **2020**, 1–12. [[CrossRef](#)] [[PubMed](#)]
4. Bratov, A.; Abramova, N.; Ipatov, A. Recent trends in potentiometric sensor arrays—A review. *Anal. Chim. Acta* **2010**, *678*, 149–159. [[CrossRef](#)] [[PubMed](#)]
5. Oleneva, E.; Savosina, J.; Agafonova-Moroz, M.; Lumpov, A.; Babain, V.; Jahatspanian, I.; Legin, A.; Kirsanov, D. Potentiometric multisensor system for tetra- and hexavalent actinide quantification in complex rare earth metal mixtures related to spent nuclear fuel reprocessing. *Sens. Actuators B Chem.* **2019**, *288*, 155–162. [[CrossRef](#)]
6. Savosina, J.; Agafonova-Moroz, M.; Yaroshenko, I.; Ashina, J.; Babain, V.; Lumpov, A.; Legin, A.; Kirsanov, D. Plutonium (IV) quantification in technologically relevant media using potentiometric sensor array. *Sensors* **2020**, *20*, 1604. [[CrossRef](#)] [[PubMed](#)]
7. Agafonova-Moroz, M.; Savosina, J.; Voroshilov, Y.; Lukin, S.; Lumpov, A.; Babain, V.; Oleneva, E.; Legin, A.; Kirsanov, D. Quantification of thorium and uranium in real process streams of mayak radiochemical plant using potentiometric multisensor array. *J. Radioanal. Nucl. Chem.* **2020**, *323*, 605–612. [[CrossRef](#)]
8. Naumova, Y.A.; Sapozhnikova, N.V.; Egorova, O.N.; Lumpov, A.A. Determination of concentrations of fission products by ICP–AES in solutions from spent nuclear fuel reprocessing. *Radiochemistry* **2017**, *59*, 618–623. [[CrossRef](#)]
9. Bryan, S.A.; Levitskaia, T.G.; Johnsen, A.M.; Orton, C.R.; Peterson, J.M. Spectroscopic monitoring of spent nuclear fuel reprocessing streams: An evaluation of spent fuel solutions via Raman, visible, and near-infrared spectroscopy. *Radiochim. Acta* **2011**, *99*, 563–572. [[CrossRef](#)]
10. Kirsanov, D.; Babain, V.; Agafonova-Moroz, M.; Lumpov, A.; Legin, A. Combination of optical spectroscopy and chemometric techniques—A possible way for on-line monitoring of Spent Nuclear Fuel (SNF) reprocessing. *Radiochim. Acta* **2012**, *100*, 185–188. [[CrossRef](#)]
11. Wilski, H. The radiation induced degradation of polymers. *Int. J. Radiat. Appl. Instrum. Part. C Radiat. Phys. Chem.* **1987**, *29*, 1–14. [[CrossRef](#)]
12. Torikai, A.; Geetha, R.; Nagaya, S.; Fueki, K. Radiation-induced degradation of polyethylene: Polymer structure and stability. *J. Polym. Sci. Part. A Polym. Chem.* **1990**, *28*, 3639–3646. [[CrossRef](#)]

13. Kubota, H. In-field behavior of and cumulative effects on certain electrodes in a gamma field. *Anal. Chem.* **1970**, *42*, 1593–1596. [[CrossRef](#)]
14. Gulens, J.; West, S.J.; Ross, J.W. Influence of high gamma radiation fields on response of ion-selective electrodes. *Anal. Chem.* **1984**, *56*, 2367–2368. [[CrossRef](#)]
15. Zarzana, C.A.; Groenewold, G.S.; Mincher, B.J.; Mezyk, S.P.; Wilden, A.; Schmidt, H.; Modolo, G.; Wishart, J.F.; Cook, A.R. A comparison of the γ -radiolysis of TODGA and T(EH)DGA using UHPLC-ESI-MS analysis. *Solvent Extr. Ion. Exch.* **2015**, *33*, 431–447. [[CrossRef](#)]
16. Harris, R.K.; Becker, E.D.; Cabral de Menezes, S.M.; Goodfellow, R.; Granger, P. NMR Nomenclature. Nuclear spin properties and conventions for chemical shifts (IUPAC recommendations 2001). *Pure Appl. Chem.* **2001**, *73*, 1795–1818. [[CrossRef](#)]